

Biogeosciences Discussions is the access reviewed discussion forum of *Biogeosciences*

**Anthropogenic CO₂
in the Atlantic Ocean**

M. Vázquez-Rodríguez et
al.

Anthropogenic carbon distributions in the Atlantic Ocean: data-based estimates from the Arctic to the Antarctic

M. Vázquez-Rodríguez¹, F. Touratier², C. Lo Monaco³, D. W. Waugh⁴,
X. A. Padin¹, R. G. J. Bellerby^{5,6}, C. Goyet², N. Metzl³, A. F. Ríos¹, and F. F. Pérez¹

¹Instituto de Investigaciones Marinas, CSIC, Eduardo Cabello 6, 36208 Vigo, Spain

²IMAGES, Université de Perpignan, 52 avenue Paul Alduy, 66860 Perpignan, France

³LOCEAN/IPSL, Université Pierre et Marie Curie, case 100, 75252 Paris cedex 05, France

⁴Department of Earth and Planetary Sciences, Johns Hopkins University, Baltimore, USA

⁵Bjerknes Centre for Climate Research, Univ. of Bergen, Allégaten 55, 5007 Bergen, Norway

⁶Geophysical Institute, University of Bergen, Allégaten 70, 5007 Bergen, Norway

Received: 4 March 2008 – Accepted: 7 March 2008 – Published: 7 April 2008

Correspondence to: M. Vázquez-Rodríguez (mvazquez@iim.csic.es)

Published by Copernicus Publications on behalf of the European Geosciences Union.

Title Page

Abstract

Introduction

Conclusions

References

Tables

Figures

◀

▶

◀

▶

Back

Close

Full Screen / Esc

Printer-friendly Version

Interactive Discussion



Abstract

Five of the most recent observational methods to estimate anthropogenic CO₂ (C_{ant}) are applied to a high-quality dataset from five representative sections of the Atlantic Ocean extending from the Arctic to the Antarctic. Between latitudes 60° N–40° S all methods give similar spatial distributions and magnitude of C_{ant}. Conversely, large discrepancies are found in the Southern Ocean and Nordic Seas. The differences in the Southern Ocean have a significant impact on the anthropogenic carbon inventories. The calculated total inventories of C_{ant} for the Atlantic referred to 1994 range from 48 to 67 Pg (10¹⁵ g) of carbon, with an average of 54±8 Pg C, which is higher than previous estimates. These results, both the detailed C_{ant} distributions and extrapolated inventories, will help to validate biogeochemical ocean models and coupled climate-carbon models.

1 Introduction

Understanding and modelling the marine carbon system is one of the most pressing issues within the framework of climate change. Carbon dioxide, an important greenhouse gas, is being increasingly produced by human activities, adding to the “natural” carbon cycle. International effort has been focussed to investigate the evolution of the oceanic sink of atmospheric CO₂, and to understand how human activities interfere in this air-sea coupled system. The endeavour aims at gaining insight on the assessment of the future possible scenarios proposed by the Intergovernmental Panel on Climate Change (IPCC Fourth Assessment Report: Climate Change 2007¹). The invasion of anthropogenic CO₂ (C_{ant}) in the ocean affects not only the atmospheric carbon dioxide concentrations and is associated to climate change, but has also a direct impact on ocean chemistry, causing the so-called “ocean acidification” (Feely et al., 2004). The

¹<http://www.ipcc.ch/>

BGD

5, 1421–1443, 2008

Anthropogenic CO₂ in the Atlantic Ocean

M. Vázquez-Rodríguez et
al.

Title Page

Abstract

Introduction

Conclusions

References

Tables

Figures

◀

▶

◀

▶

Back

Close

Full Screen / Esc

Printer-friendly Version

Interactive Discussion



largest ocean acidification upshots for the environment are expected to occur in the high northern and southern latitudes (Bellerby et al., 2005; Orr et al., 2005).

In this context, estimating C_{ant} concentrations in the oceans represents an important step towards a better evaluation of the global carbon budget and its changes. Since

C_{ant} may not be directly measured in the ocean it has to be derived from in-situ observations, under several assumptions. The pioneering original works by Brewer (1978) and Chen and Millero (1979) addressed this issue, and estimated C_{ant} in sub-surface water masses of the Atlantic Ocean from total inorganic carbon (C_T) measurements. They corrected the measured C_T for the biological contribution and made an estimate of the preformed Preindustrial C_T (C_T when the water was last in contact with the 1850 atmosphere) that was also subtracted from the observed C_T . In the last ten years, several observational (data-based) methods have been investigated at regional and global scales (see Wallace et al., 2001, for a historical overview). Two of them, the ΔC^* method (Gruber et al., 1996) and the Transient Time Distribution (TTD) method (Hall et al., 2002) have been applied at global scale. By using the ΔC^* approach, Sabine et al. (2004) estimated a global oceanic inventory of C_{ant} for a nominal year of 1994 of $118 \pm 19 \text{ Pg C}$, which represents about 50% of the fossil fuel CO_2 emitted between 1800 and 1994. Similarly, Waugh et al. (2006) applied the TTD method to estimate the C_{ant} inventory for the global ocean and obtained results ranging between 94 and 121 Pg C for 1994. These authors also compared the C_{ant} distribution derived from the ΔC^* and TTD approaches and pointed out that in spite of the grand-scale reasonable agreement, substantial differences occurred in the North Atlantic, South-Eastern Atlantic and in all basins South of 30°S . This was an important result as it offered a range of C_{ant} concentrations to be used as a benchmark to be checked with ocean carbon cycle models. Analogous results were derived from intercomparison studies with Ocean General Circulation Models (OGCM) (Orr et al., 2001), i.e.: reasonable agreement was found for ocean-wide inventories but significant differences prevailed at a regional scale in terms of inventory and as to where C_{ant} was actually located, especially in the high latitudes and between the upper and lower ocean.

Anthropogenic CO_2 in the Atlantic Ocean

M. Vázquez-Rodríguez et
al.

Title Page

Abstract

Introduction

Conclusions

References

Tables

Figures

◀

▶

◀

▶

Back

Close

Full Screen / Esc

Printer-friendly Version

Interactive Discussion



**Anthropogenic CO₂
in the Atlantic Ocean**

M. Vázquez-Rodríguez et
al.

Title Page

Abstract

Introduction

Conclusions

References

Tables

Figures

◀

▶

◀

▶

Back

Close

Full Screen / Esc

Printer-friendly Version

Interactive Discussion



In more recent years, additional data-based methods were developed in an attempt to improve the existing oceanic C_{ant} estimates, especially at a regional level. These are the TrOCA method (Touratier and Goyet, 2004; Touratier et al., 2007), the C_{IPSL}° method (Lo Monaco et al., 2005a) and the φC_T° method (Vázquez-Rodríguez et al., 2008²). To date, only few of these observational methods, including the ΔC^* , have been objectively inter-compared, and that is at regional scales only, namely: in the North Atlantic (Wanninkhof et al., 1999; Friis et al., 2006; Tanhua et al., 2007), the North Indian (Coatanoan et al., 2001), or along a single section in the Southern Ocean (Lo Monaco et al., 2005b). All of these studies identified significant discrepancies in C_{ant} distributions and specific inventories depending on the location, set of compared C_{ant} estimation approaches and methodological assumptions.

Today, there is a pressing need to compare and clarify the C_{ant} estimates from these various observational methods, as it has been analogously addressed in the case of ocean carbon models (OCMIP project; Orr et al., 2001), atmospheric inverse models (Gurney et al., 2004), or coupled climate-carbon models (C4MIP project³). As a contribution to the European integrated project of CARBOOCEAN, this international collaborative study will focus on the comparison of results from five different concepts used to estimate anthropogenic CO₂ concentrations from a single and common high-quality data set in the Atlantic Ocean, including the Arctic and Southern Ocean sectors. The results will give insight over the uncertainties attached to these C_{ant} calculation procedures. They will also serve observational and numerical ocean modellers to validate their simulations and will help to reach a consensus as to where C_{ant} is captured and actually stored. Our analysis investigates the high latitudes (Southern Ocean and Nordic Seas) as locations where uncertainties are expected to be large for both data-based methods (Lo Monaco et al., 2005b; Waugh et al., 2006) and OGCMs (Orr et

²Vázquez-Rodríguez, M., Padin, X. A., Pérez, F. F., Ríos, A. F., and Bellerby, R. G. J.: Anthropogenic carbon determination from sub-surface boundary conditions, Deep-Sea Res., under review, 2008.

³<http://www.atmos.berkeley.edu/c4mip/>

al., 2001). The Atlantic Ocean has been selected here because it has the largest C_{ant} specific inventory of all ocean basins, and also because of its large meridional and zonal gradients of C_{ant} (Sabine et al., 2004; Waugh et al., 2006). The paper first describes the various C_{ant} meridional and zonal distributions, according to the different methods applied, focusing on key areas (water masses formation and transformation). The specific and total C_{ant} inventories are then presented and discussed on the basis of the main assumptions from the methods as possible sources for the observed dissimilarities.

2 Method

Data from four selected meridional sections (NSeas-Knorr, CLIVAR A16N, WOCE I06-Sb and WOCE A14) cover the length of the Atlantic and give a representative coverage of it (Fig. 1a). The WOCE AR01 extends from the Atlantic east to west ends at $\sim 24^\circ$ N (Fig. 2a). They have all been recently conducted within the framework of either the WOCE or CLIVAR programs, except for the cruise in the Nordic Seas (NSeas, 2005) on board the R/V Knorr (Bellerby et al., 2005; Olsen et al., 2006). The data are available from the GLODAP website⁴, except for the NSeas data⁵ and the CLIVAR repeat section A16N legs 1 and 2 conducted during 2003⁶.

Five data-based methods for C_{ant} estimation have been considered in this study: the TTD, the TrOCA, the C_{IPSL}° and the φC_T° . The ΔC^* method has also been included in this comparison, but it has not been applied to the same data-set. The C_{ant} results here shown correspond to the same cruises though (except for the NSeas-Knorr one), taken from the C_{ant} appearing in the GLODAP dataset as of Lee et al. (2003). They have applied the ΔC^* method to evaluate the inventory of C_{ant} in the Eastern and

⁴http://cdiac.ornl.gov/oceans/glodap/Glodap_home.htm

⁵http://cdiac.ornl.gov/ftp/oceans/CARINA/316N20020601_data/

⁶http://www.clivar.org/carbon_hydro/hydro_table.php

Anthropogenic CO_2 in the Atlantic Ocean

M. Vázquez-Rodríguez et
al.

Title Page

Abstract

Introduction

Conclusions

References

Tables

Figures

◀

▶

◀

▶

Back

Close

Full Screen / Esc

Printer-friendly Version

Interactive Discussion



Western basins of the Atlantic. Their C_{ant} estimates have been included in the global synthesis of Sabine et al. (2004) and the GLODAP database (Key et al., 2004).

The methods can be classified into two groups on the basis of the variables needed to compute C_{ant} : a) the Carbon-based methods (ΔC^* , C_{IPSL}° , TrOCA, and φC_T°), which typically require measurements of dissolved inorganic carbon (C_T), total alkalinity (A_T), oxygen, temperature, salinity and eventually some nutrient analysis; b) the Transient-Tracer-based methods (TTD) that commonly use CFC-11 or CFC-12 concentration measurements as proxies of the anthropogenic CO_2 signal.

3 Results and discussion

3.1 Anthropogenic CO_2 distributions

The meridional distributions of C_{ant} calculated from the ΔC^* , φC_T° , C_{IPSL}° , TrOCA, and TTD methods are shown in Fig. 1d–h, respectively. As the data were collected in different years, the C_{ant} results have been referred to a single common year (1994) to eliminate biases introduced by the increasing atmospheric $f\text{CO}_2$. This was done using data from time series of CO_2 molar fractions ($x\text{CO}_2$) and calculating from here the annual rate of increase of C_{ant} at the year each cruise was conducted (Mikaloff-Fletcher et al., 2006). This correction typically varied between $1\text{--}7 \mu\text{mol kg}^{-1}$ of C_{ant} . Another consideration has been the overlapping latitudes of the A16N-A14 and A14-I06Sb section pairs. The general selection criteria followed was choosing the stations that were deepest and had the least influence of Indian Ocean waters. Accordingly, the northernmost ends of the A14 and I06Sb cruises are omitted from the plots (Fig. 1a). Finally, negative C_{ant} estimates that were within the specific range of uncertainty in each method were set to zero (ad hoc), while values more negative than that were taken as outliers and excluded from subsequent analysis.

All C_{ant} distributions in Fig. 1 share raw similarities in the patterns, most noticeably in the area of largest gradient, above the $15 \mu\text{mol kg}^{-1}$ isopleth. The strong water mass

BGD

5, 1421–1443, 2008

Anthropogenic CO_2 in the Atlantic Ocean

M. Vázquez-Rodríguez et
al.

Title Page

Abstract

Introduction

Conclusions

References

Tables

Figures

◀

▶

◀

▶

Back

Close

Full Screen / Esc

Printer-friendly Version

Interactive Discussion



Anthropogenic CO₂ in the Atlantic Ocean

M. Vázquez-Rodríguez et
al.

Title Page

Abstract

Introduction

Conclusions

References

Tables

Figures

◀

▶

◀

▶

Back

Close

Full Screen / Esc

Printer-friendly Version

Interactive Discussion



formation processes in the North Atlantic subpolar gyre (Schmitz, 1996) have a large effect on the dynamics of C_{ant} oceanic uptake. These cause the different C_{ant} distributions observed in the Nordic Seas, where the $15 \mu\text{mol kg}^{-1}$ isoline shallows abruptly. The maximum C_{ant} values ($40\text{--}60 \mu\text{mol kg}^{-1}$) are consistently located in the northern subtropical gyre [20°N , 50°N], where the intensification of the Meridional Overturning Circulation (MOC) also provokes the strongest water mass outcrops and deepest C_{ant} transport. Alternatively, C_{ant} minima are quite unanimously located under the southern subtropical gyre below 1500 m, within the oldest water masses found on the Atlantic north-eastern basin (Figs. 1b, 2b). The results for the WOCE AR01 cruise (Fig. 2) show a similar degree of agreement to the meridional section just described. There are three distinctive features in the AR01 section: a) The first 1000 m are characterised by a strong vertical C_{ant} gradient, from 60 to $20 \mu\text{mol kg}^{-1}$; b) The minimum values ($0\text{--}15 \mu\text{mol kg}^{-1}$) are consistently located in the eastern Atlantic Basin; c) The entrainment eastwards of the Deep Western Boundary Current (DWBC) upper limb is detected unanimously at ~ 1500 m, whereas its lower limb is not always as evidently marked.

In spite of the large-scale C_{ant} distribution similarities, there are significant differences, most notably in the Antarctic Bottom Water (AABW) and the Nordic Seas. The regions highlighted in Figs. 1b and 2b (boxes 1–5) and listed in Table 1 indicate the places where the focus of analysis goes. Whenever two or more results from different methods are compared within a region, a hypothesis contrast is applied with confidence level $\alpha=0.05$, considering the number of data (N) and using the population means of the standard errors of the mean (σ/\sqrt{N}).

3.1.1 Deep South Atlantic

The oldest water masses in the Atlantic are found in deep waters around 30°S and they are expected to have near-zero C_{ant} loads (Fig. 1b, Table 1). All methods yield very low values, with ΔC^* and C_{IPSL}° estimates the smallest and TTD and ϕC_T° the

largest. Most ΔC^* estimates for this region were either missing values or outliers and, therefore, excluded for inventory computations. In addition the ΔC^* method defines its absolute zero- C_{ant} reference at the deep, very old waters based on CFC or $\Delta^{14}\text{C}$ age estimates. Analogous comments apply to the results from the C_{IPSL}° method, although this one does not report as many negative or missing values as in the ΔC^* case.

3.1.2 Subtropical gyres

The northern subtropical gyre, with an observed average age of 4 years (left-hand Box 2 in Fig. 1b), contains the maximum C_{ant} values. Compared to the TTD estimates the Carbon-based methods TrOCA, C_{IPSL}° and φC_T° are all found to be significantly (but not dramatically) higher (p-level > 0.995 in all cases). The effect that the biology of the region could introduce via the oxygen to carbon ratio (R_C) is likely to have a minimum impact on the Carbon-based methods results, given the low apparent oxygen utilisation (AOU) average values. Alternatively, the average ΔC^* estimate is significantly lower than the TTD ones by $-3.3 \mu\text{mol kg}^{-1}$ (Table 1). A benchmark against which all these near-surface C_{ant} estimates can be compared is the theoretical $C_{\text{ant}}^{\text{sat}}$ saturation concentration for an ocean in equilibrium with the atmosphere in 1994 ($C_{\text{ant}}^{\text{sat}}$). Considering the average salinity and temperature of the northern subtropical gyre (Table 1) $C_{\text{ant}}^{\text{sat}}$ is estimated to be $49 \mu\text{mol kg}^{-1}$. This value is close to the average estimates from all methods except for the ΔC^* approach. On the contrary, in the southern subtropical gyre the TTD and ΔC^* estimates show no significant differences, and are the closest values to $C_{\text{ant}}^{\text{sat}}$ for this region ($46 \mu\text{mol kg}^{-1}$). The TrOCA and φC_T° results are 6 and $2.4 \mu\text{mol kg}^{-1}$ lower than the TTD, while the C_{IPSL}° is the highest value recorded ($52.3 \mu\text{mol kg}^{-1}$). Regarding the southern subtropical gyre (left-hand Box 2 in Fig. 1b), the different C_{ant} estimates compare analogously to its northern counterpart, but with slightly lower concentrations over the region and lesser C_{ant} entrainment into the ocean interior. Lastly, it is worth noting that all methods detect the Mediterranean Water (MW) influence, which causes a relative maximum of C_{ant} (average $22.6 \pm 3.5 \mu\text{mol kg}^{-1}$) at

Anthropogenic CO_2 in the Atlantic Ocean

M. Vázquez-Rodríguez et al.

Title Page

Abstract

Introduction

Conclusions

References

Tables

Figures

◀

▶

◀

▶

Back

Close

Full Screen / Esc

Printer-friendly Version

Interactive Discussion



about 1100 m depth at 37° N (Ríos et al., 2001; Álvarez et al., 2005).

3.1.3 The Southern Ocean

South of 50° S the different methods, although applied to the same dataset, present very contrasting results. The AABW forms in this region from Circumpolar Deep Water (CDW) and Ice Shelf Waters (ISW), potentially driving in the Southern Ocean an intense conveyance of C_{ant} down to the seafloor (>5000 m). The fact that C_{ant} may have penetrated this far down in the Southern Ocean is also suggested by the presence of CFC-12 in the water column (box 3 in Fig. 1b). Consequently, the TTD method (based mainly on CFCs) produced C_{ant} down to the bottom at high latitudes, a signal that was not captured in the ΔC^* results (Lo Monaco et al., 2005a, b; Waugh et al., 2006). Interestingly, the other methods (TrOCA, C_{IPSL}° and φC_T°) also detected significant C_{ant} concentrations in the deep and bottom waters of the Southern Ocean. The ΔC^* predictions give close-to-zero C_{ant} values ($1.5 \pm 1.6 \mu\text{mol kg}^{-1}$) and are clearly lower than other estimates. The ΔC^* method assigns by default $C_{\text{ant}}=0$ references to old, low CFC concentration waters like those found below depths of 500 m in the neighbouring regions of the South Atlantic (Gruber et al., 1996). Also, the ΔC^* approach assumes oxygen saturation in surface waters. The low results obtained in this area could follow from this assumption (Lo Monaco et al., 2005a). Nevertheless, it must be noted that authors like Sabine et al. (2002), by applying the ΔC^* method in other sectors of the Southern Ocean, have obtained higher C_{ant} estimates. Alternatively, the fact that the Southern Ocean is a large volume of water makes small differences between methods translate into significant inventory differences in this region (Lo Monaco et al., 2005b).

3.1.4 The Nordic Seas

Here only four methods are compared since the GLODAP data-set (i.e., the ΔC^* method) did not include the 2005 NSeas-Knorr data used in this study. In the upper layer (100–750 m, upper Box 4 in Fig. 1b), the C_{IPSL}° approach gives the high-

BGD

5, 1421–1443, 2008

Anthropogenic CO₂ in the Atlantic Ocean

M. Vázquez-Rodríguez et
al.

Title Page

Abstract

Introduction

Conclusions

References

Tables

Figures

◀

▶

◀

▶

Back

Close

Full Screen / Esc

Printer-friendly Version

Interactive Discussion



est estimate ($38.2 \pm 1.1 \mu\text{mol kg}^{-1}$) followed by the TTD ($28.1 \pm 0.5 \mu\text{mol kg}^{-1}$), while the TrOCA and φC_T° methods give lower and similar values ($24.2 \pm 1.4 \mu\text{mol kg}^{-1}$ and $23.2 \pm 1.1 \mu\text{mol kg}^{-1}$, respectively). In the lower Nordic Seas (1500 m to bottom, lower Box 4 in Fig. 1b), all four methods produced different results and the discrepancies are larger than in the upper region: estimates from the TrOCA ($4.1 \pm 1.2 \mu\text{mol kg}^{-1}$) and φC_T° ($6.4 \pm 0.8 \mu\text{mol kg}^{-1}$) approaches are statistically lower, almost by half, than the TTD results. The C_{IPSL}° method gives the maximum C_{ant} estimate ($20.9 \pm 1.1 \mu\text{mol kg}^{-1}$), almost twice as large as the TTD method average value ($11.3 \pm 0.5 \mu\text{mol kg}^{-1}$), that is, about the same differences observed in the deep Southern Ocean.

3.1.5 The Deep Western Boundary Current (DWBC)

This current is detected in Fig. 2 by all methods. The difference between methods comes from the intensity with which the vertical C_{ant} gradient generated by the upper (uDWBC) and lower (IDWBC) limbs is detected. The clearest DWBC signal is given by the C_{IPSL}° method, whilst the signal from the TTD approach is the weakest in terms of eastward penetration and vertical gradient between the two limbs. The TrOCA and ΔC^* methods display the largest gradient between limbs. However, when we compared the signal from the eastward entrainment of the IDWBC from both methods the TrOCA showed a well-defined limb, while the ΔC^* one is almost imperceptible. The φC_T° method gives values that fall half-range from all methods (Table 1) but has a weak IDWBC signal that is reproduced slightly deeper than in the rest of methods. Finally, it is also remarkable that the eastward deflection and propagation of the North Atlantic Deep Water upper limb (uNADW) coming from the uDWBC (Weiss et al., 1985; Andrié et al., 1998) can also be observed in Fig. 1: a C_{ant} maximum located at 1500–2000 m depth in the Equator, corresponding with a relative CFC12 age minimum of ~ 50 years is detected to different extents by all methods.

Overall, the largest discrepancies are found to occur in the high latitudes, most im-

Anthropogenic CO_2 in the Atlantic Ocean

M. Vázquez-Rodríguez et
al.

Title Page

Abstract

Introduction

Conclusions

References

Tables

Figures

◀

▶

◀

▶

Back

Close

Full Screen / Esc

Printer-friendly Version

Interactive Discussion



importantly in the Southern Ocean due to its larger contribution to Atlantic inventories compared with the Nordic Seas, as discussed next.

3.2 Atlantic inventories of anthropogenic CO₂

To assess how the above-described convergences and discrepancies of the various data-based C_{ant} estimates would affect the global C_{ant} budget, we integrated the results on the Atlantic basin scale. For this, the water column integration has been grouped into the same 10-degree wide latitude bands as in Lee et al. (2003). This way, their results could be added as representatives of the ΔC* method to those calculated here. A few considerations made regarding inventory computations: a) To avoid the seasonal biogeochemical variability from surface layer data, no in situ surface individual C_{ant} estimates were used. Instead, values from the bottom limit of the winter mixed-layer were extended to 0 m, so that C_{ant} from surface waters is still being considered in inventory calculations (Lo Monaco et al., 2005b). On the basis of winter mixed layer depths, the location of the bottom limits were placed at 100 m in subtropical and equatorial waters, and at 300 m for waters in the [33° S–50° S] latitude band; b) Regarding total inventories, the meridional cruises used in this study belong to the Eastern Atlantic basin. To tackle the zonal asymmetry assumption, results in Table 5 from Lee et al. (2003) were used. They provided specific inventories (mol m⁻²) for the eastern and western basins and the total inventories (Pg C) for different latitude bands. A conversion factor per band of latitude (1.04±0.10) that accounted for the area was calculated using the eastern basin specific inventory and the total inventory data from Lee et al. (2003); c) The C_{ant} inventories from Gruber (1998) and Lee et al. (2003) are included in Fig. 3a) to show how the ΔC* method yields very low values in the Southern Ocean, regardless of the dataset to which it is applied (Lo Monaco et al., 2005a). These inventories were calculated from different data collected over the same region here studied, and were referenced to year 1994; d) The errors for the specific inventories are of ±1 mol m⁻² and ±2 mol m⁻² when integrated down to 3000 m or 6000 m, respectively. They were calculated by means of random propagation of a 5 μmol kg⁻¹ standard error of the C_{ant}

Anthropogenic CO₂ in the Atlantic Ocean

M. Vázquez-Rodríguez et
al.

Title Page

Abstract

Introduction

Conclusions

References

Tables

Figures

◀

▶

◀

▶

Back

Close

Full Screen / Esc

Printer-friendly Version

Interactive Discussion



estimate with depth. Error bars in Fig. 3a are omitted for clarity.

All methods give reasonably similar specific inventories (Fig. 3a), except for the ΔC^* method as of either Gruber (1998) or Lee et al. (2003) in the Southern Ocean. The greatest similarities occur in the subtropical and equatorial regions, while some discrepancies between the C_{IPSL}° , φC_T° , TrOCA and TTD methods appear towards higher latitudes, especially north from 55° N, where none of the predictions converges. In the Southern Ocean (south of 55° S), the ΔC^* method shows extremely low values ($10 \pm 5 \text{ mol m}^{-2}$ on average) considering the non-negligible amount of CFCs found in this basin (Fig. 1b). These estimates are five to seven times lower than any other result in this area. The strong decreasing trend of the specific inventories according to the ΔC^* approach is also opposite to the rest of Carbon-based methods which describe increasing specific inventories south of 45° S. We also identified substantial differences in other regions: In the tropics, the TTD method gives about half the amount of C_{ant} the C_{IPSL}° method does, and in the North Atlantic differences of 20 mol m^{-2} are common.

The specific inventories were integrated by area to calculate the total inventories (in Pg C) over the same bands of latitude (Fig. 3b). In so doing, the aforementioned differences in the Nordic Seas diminish. All methods display an “M-shape” in the total inventory latitudinal distribution, with a coherent maximum around $20\text{--}30^\circ$ N and a relative maximum at $40\text{--}50^\circ$ S. Although significant differences are still identified between methods, we believe that the “M-shape” describes faithfully oceanic anthropogenic CO_2 fields and should be reproduced by ocean and climate models. The total inventories for the Atlantic basin (excluding the Nordic Seas), referred to 1994 estimated by the C_{IPSL}° , φC_T° , TrOCA and TTD methods are: 67, 55, 51 and 48 Pg C, respectively (average $55 \pm 8 \text{ Pg C}$). In any case, these results are higher than the 47 Pg C inventory given by Lee et al. (2003) using the ΔC^* approach. This would lower the average inventory of the Atlantic to $54 \pm 8 \text{ Pg C}$. The main reason for the low inventory from the ΔC^* method comes mainly from the low C_{ant} concentrations predicted in the Southern Ocean (Fig. 1d), which alone represents 11–12% of the total inventory. The average C_{ant} inventories for the North and South Atlantic, considering all five methods, are

BGD

5, 1421–1443, 2008

Anthropogenic CO_2 in the Atlantic Ocean

M. Vázquez-Rodríguez et
al.

Title Page

Abstract

Introduction

Conclusions

References

Tables

Figures

◀

▶

◀

▶

Back

Close

Full Screen / Esc

Printer-friendly Version

Interactive Discussion



32±4 Pg C and 22±5 Pg C, respectively.

3.3 Discussion

The discrepancies in the total inventories are mainly explained from the results obtained for waters under the 5°C isotherm (Fig. 1c), which separates ~86% of the Atlantic volume (excluding marginal seas) and divides the C_{ant} inventory by approximately half. This means that small errors in the estimation of C_{ant} have larger impacts in the inventories when they occur in $\theta < 5^\circ\text{C}$ waters, and has direct consequences intrinsic to the assumptions in each data-based method. For instance, the high estimates obtained with the C_{IPSL}° method in the Southern Hemisphere can derive from having overestimated the oxygen undersaturation in Antarctic surface waters, which would lead to C_{ant} overestimates (Lo Monaco et al., 2005a). For the TrOCA method we identified low inventory estimates in the South Atlantic (Fig. 3b) due to the relatively large amount of negative C_{ant} estimates in deep waters (Fig. 1g). The TTD method gives the lowest total inventory in the North Atlantic. This approach assumes a global constant mixing to advection ratio of $\Delta/\Gamma = 1$ and this constraint might not be representative of the North Atlantic. Here, the influence of the MOC makes advection gain importance over the mixing processes. Finally, the φC_T° method lacks extreme values at virtually any of the studied regions, although slightly low values are found in the upper 1000 m of the Nordic Seas.

The assumptions made by the methodologies suggest that the causes for the disagreements may be due to: a) Ice cap hindering of ventilation processes that alter the source properties of the water masses; b) The Alkalinity signal from the Arctic rivers is very different to the other waters of the world ocean; c) Surface layer observations are normally used to parameterize properties, like preformed A_T (A_T° , i.e., A_T at the moment the water mass outcrops) or air-sea CO_2 disequilibrium (ΔC_{dis}), that are later conveyed to the underlying isopycnals. The climate-change-driven shift of surface thermal characteristics would force the parameterizations to propagate wrong values towards the deeper ends of isopycnals, which have not sensed this thermal alteration

BGD

5, 1421–1443, 2008

Anthropogenic CO_2 in the Atlantic Ocean

M. Vázquez-Rodríguez et
al.

Title Page

Abstract

Introduction

Conclusions

References

Tables

Figures

◀

▶

◀

▶

Back

Close

Full Screen / Esc

Printer-friendly Version

Interactive Discussion



yet. d) The North Atlantic Central Water (NACW) enters the surface North Atlantic and Norwegian Atlantic Current Systems with higher loads of anthropogenic CO_2 than they did in the past. This process causes the ΔC_{dis} driving C_{ant} uptake to diminish (Olsen et al., 2006). These factors introduce biases in the equations used to calculate C_{ant} .

In spite of the general convergence of the methods considered the choice of one data-based approach or another really depends on the region of interest, given the local variability of the results (Table 1, Fig. 3). Future revisions of the methods should focus on improving C_{ant} estimates in the Southern Ocean and Nordic Seas. These areas seem to be a determining issue in the discrepancies found for anthropogenic CO_2 burdens. The approximations of constant R_C ratios made by all Carbon-based methods and the same relative weight given to advection and mixing ($\Delta/\Gamma=1$ (Waugh et al., 2006)) at a global scale by the TTD method need to be relaxed. Finally, all methods should strive to improve their own implementation of the intricate mixing issues in strong water mass formation regions, particularly in the Northern Subpolar Gyre and Nordic Seas.

4 Conclusion

The TTD, ΔC^* , TrOCA, C_{IPSL}° and φC_7° observational methods have produced satisfactory C_{ant} estimates and inventories for the full length of the Atlantic Ocean. The uncertainties in C_{ant} estimates due to the method applied are narrow in the subtropics but larger for polar regions. The impact of these discrepancies is most important in the Southern Ocean given its large contribution (up to 12%) to the total inventory of C_{ant} . The average C_{ant} Atlantic inventory of $54 \pm 8 \text{ Pg C}$ here obtained from the five methods suggests that previous results given by Gruber (1998) and Lee et al. (2003) could be underestimating Atlantic C_{ant} loads. Adding to the basin-scale intercomparison here performed, regional validation is encouraged for modellers since similar Atlantic inventories could result from diverse C_{ant} distributions, as shown here. It is worth noting that the large uncertainties in C_{ant} distribution identified in the Southern Ocean and Nordic

BGD

5, 1421–1443, 2008

Anthropogenic CO_2 in the Atlantic Ocean

M. Vázquez-Rodríguez et
al.

Title Page

Abstract

Introduction

Conclusions

References

Tables

Figures

◀

▶

◀

▶

Back

Close

Full Screen / Esc

Printer-friendly Version

Interactive Discussion



Seas could lead to diverse scenarios and, henceforth, different conclusions regarding issues such as the carbon system saturation state and ocean acidification. Therefore, a multi data-based analysis combining outputs from observational and numerical models at different scales is strongly encouraged and should be addressed in the future.

5 The results here shown will also help to better understand the evolution of the latitudinal atmospheric CO₂ gradient since the Preindustrial era, and how this is associated with the meridional transports of C_T on the long-time scale.

Acknowledgements. We would like to extend our gratitude to the Chief Scientists, scientists and crew who participated and put their effort in the oceanographic cruises utilized in this study, particularly to those responsible for the carbon, CFC, and nutrients measurements. This work was developed and funded by the European Commission within the 6th Framework Programme (EU FP6 CARBOOCEAN Integrated Project, Contract no. 511176). M. Vázquez-Rodríguez is funded by Consejo Superior de Investigaciones Científicas (CSIC) I3P predoctoral grant program REF. I3P-BPD2005.

15 References

Álvarez, M., Pérez, F. F., Shoosmith, D. R., and Bryden, H. L.: The unaccounted role of Mediterranean Water in the draw-down of anthropogenic carbon, *J. Geophys. Res.*, 110, 1–18, doi:10.1029/2004JC002633, 2005.

Andrié, C., Ternon, J. F., Messias, M. J., Mémerly, L., and Bourlès, B.: Chlorofluoromethanes distributions in the deep equatorial Atlantic during January–March 1993, *Deep-Sea Res. I*, 45, 903–930, 1998.

Bellerby, R. G. J., Olsen, A., Furevik, T., and Anderson, L. A.: Response of the surface ocean CO₂ system in the Nordic Seas and North Atlantic to climate change, in: *Climate Variability in the Nordic Seas*, edited by: Drange, H., Dokken, T. M., Furevik, T., Gerdes, R., and Berger, W., *Geophysical Monograph Series, AGU*, 189–198, 2005.

Brewer, P. G.: Direct observation of the oceanic CO₂ increase, *Geophys. Res. Lett.*, 5, 997–1000, 1978.

Chen, C.-T. A. and Millero, F. J.: Gradual increase of oceanic CO₂, *Nature*, 277, 205–206, 1979.

BGD

5, 1421–1443, 2008

Anthropogenic CO₂ in the Atlantic Ocean

M. Vázquez-Rodríguez et
al.

Title Page

Abstract

Introduction

Conclusions

References

Tables

Figures

◀

▶

◀

▶

Back

Close

Full Screen / Esc

Printer-friendly Version

Interactive Discussion



Coatanoan, C., Goyet, C., Sabine, C. L., and Warner, M.: Comparison of the two approaches to quantify anthropogenic CO₂ in the ocean: results from the northern Indian, *Global Biogeochem. Cycles*, 15, 11–26, 2001.

Feely, R. A., Sabine, C. L., Lee, K., Berelson, W., Kleypas, J., Fabry, V. J., Millero, F. J.: Impact of Anthropogenic CO₂ on the CaCO₃ System in the Oceans, *Science*, 305, 362–366, 2004.

Friis, K.: A review of marine anthropogenic CO₂ definitions: Introducing a thermodynamic approach based on observations, *Tellus B*, 58B, 2–15, doi:10.1111/j.1600-0889.2005.00173.x, 2006.

Gruber, N.: Anthropogenic CO₂ in the Atlantic Ocean, *Global Biogeochemical Cycles*, 12, 165–191, 1998.

Gruber, N., Sarmiento, J. L., and Stocker, T. F.: An improved method for detecting anthropogenic CO₂ in the oceans, *Global Biogeochem. Cycles*, 10, 809–837, 1996.

Hall, T. M., Haine, T. W. N., and Waugh, D. W.: Inferring the concentration of anthropogenic carbon in the ocean from tracers, *Global Biogeochem. Cycles*, 16(4), 1131, doi:10.1029/2001GB001835, 2002.

Key, R. M., Kozyr, A., Sabine, C. L., Lee, K., Wanninkhof, R., Bullister, J. L., Feely, R. A., Millero, F. J., Mordy, C., and Peng, T.-H.: A global ocean carbon climatology: Results from Global Data Analysis Project (GLODAP), *Global Biogeochem. Cycles*, 18, GB4031, doi:10.1029/2004GB002247, 2004.

Lee, K., Choi, S.-D., Park, G.-H., Wanninkhof, R., Peng, T.-H., Key, R. M., Sabine, C. L., Feely, R. A., Bullister, J. L., Millero, F. J., Kozyr, A.: An updated anthropogenic CO₂ inventory in the Atlantic Ocean, *Global Biogeochem. Cycles*, 17(4), 1116, doi:10.1029/2003GB002067, 2003.

Lo Monaco, C., Metzl, N., Poisson, A., Brunet, C., and Schauer, B.: Anthropogenic CO₂ in the Southern Ocean: Distribution and inventory at the Indian-Atlantic boundary (World Ocean Circulation Experiment line I6), *J. Geophys. Res.*, 110, C06010, doi:10.1029/2004JC002643, 2005a.

Lo Monaco, C., Goyet, C., Metzl, N., Poisson, A., and Touratier, F.: Distribution and inventory of anthropogenic CO₂ in the Southern Ocean: Comparison of three data-based methods, *J. Geophys. Res.*, 110, C09S02, doi:10.1029/2004JC002571, 2005b.

Matsumoto, K. and Gruber, N.: How accurate is the estimation of anthropogenic carbon in the ocean? An evaluation of the ΔC^* method, *Global Biogeochem. Cycles*, 19, GB3014, doi:10.1029/2004GB002397, 2005.

BGD

5, 1421–1443, 2008

Anthropogenic CO₂ in the Atlantic Ocean

M. Vázquez-Rodríguez et
al.

Title Page

Abstract

Introduction

Conclusions

References

Tables

Figures

◀

▶

◀

▶

Back

Close

Full Screen / Esc

Printer-friendly Version

Interactive Discussion



Mikaloff-Fletcher, S. E., Gruber, N., Jacobson, A. R., Doney, S. C., Dutkiewicz, S., Gerber, M., Follows, M., Joos, F., Lindsay, K., Menemenlis, D., Mouchet, A., Müller, S. A., and Sarmiento, J. L.: Inverse estimates of anthropogenic CO₂ uptake, transport, and storage by the ocean, *Global Biogeochem. Cycles*, 20, GB2002, doi:10.1029/2005GB002530, 2006.

5 Olsen, A., Omar, A. M., Bellerby, R. G. J., Johannessen, T., Ninnemann, U., Brown, K. R., Olsson, K. A., Olafsson, J., Nondal, G., Kivimäe, C., Kringstad, S., Neill, C., and Olafsdottir, S.: Magnitude and origin of the anthropogenic CO₂ increase and 13C Suess effect in the Nordic seas since 1981, *Global Biogeochem. Cycles*, 20, GB3027, doi:10.1029/2005GB002669., 2006.

10 Orr, J. E., Maier-Reimer, E., Mikolajewicz, U., Monfray, P., Sarmiento, J. L., Toggweiler, J. R., Taylor, N. K., Palmer, J., Gruber, N., Sabine, C. L., LeQuéré, C., Key, R. M., and Boutin, J.: Estimates of anthropogenic carbon uptake from four three-dimensional global ocean models, *Global Biogeochem. Cycles*, 15(1), 43–60, 2001.

Orr, J. E., Fabry, V. J., Aumont, O., Bopp, L., Doney, S. C., Feely, R. A., et al.: Anthropogenic ocean acidification over the twenty-first century and its impact on calcifying organisms, *Nature*, 437(7059), 681–686, doi:10.1038/nature04095. ISSN 0028-0836, 2005.

Ríos, A. F., Pérez, F. F., and Fraga, F.: Long term (1977–1997) measurements of carbon dioxide in the Eastern North Atlantic: evaluation of anthropogenic input, *Deep-Sea Res. II*, 48, 2227–2239, 2001.

20 Sabine, C. L., Feely, R. A., Gruber, N., Key, R. M., Lee, K., Bullister, J. L., Wanninkhof, R., Wong, C. S., Wallace, D. W. R., Tilbrook, B., Millero, F. J., Peng, T.-H., Kozyr, A., Ono, T., Ríos, A. F.: The oceanic sink for anthropogenic CO₂, *Science*, 305, 367–371, 2004.

Schmitz Jr., W. J.: On the World Ocean Circulation: Volume I, Some Global Features/North Atlantic Circulation, Woods Hole Oceanographic Institution Technical Report WHOI-96-03, 1996.

25 Sonnerup, R. E.: On the relations among CFC derived water mass ages, *Geophys. Res. Lett.*, 28, 1739–1742, 2001.

Touratier, F. and Goyet, C.: Applying the new TrOCA approach to estimate the distribution of anthropogenic CO₂ in the Atlantic Ocean, *J. Mar. Syst.*, 46, 181–197, 2004.

30 Touratier, F., Azouzi, L., and Goyet, C.: CFC-11, Δ14C and 3H tracers as a means to assess anthropogenic CO₂ concentrations in the ocean, *Tellus*, 59B, 318–325, doi:10.1111/j.1600-0889.2006.00247.x, 2007.

Touratier, F. and Goyet, C.: Applying the new TrOCA approach to assess the distribution of

BGD

5, 1421–1443, 2008

Anthropogenic CO₂ in the Atlantic Ocean

M. Vázquez-Rodríguez et
al.

Title Page

Abstract

Introduction

Conclusions

References

Tables

Figures

◀

▶

◀

▶

Back

Close

Full Screen / Esc

Printer-friendly Version

Interactive Discussion



anthropogenic CO₂ in the Atlantic Ocean, *J. Mar. Syst.*, 46, 181–196, 2007.

Wallace, D. W. R.: Storage and transport of excess CO₂ in the oceans: the JGOFS/WOCE global CO₂ survey, in: *Ocean Circulation and Climate*, edited by: Siedler, G., Church, J., and Gould, J., Academic Press, San Diego, USA, pp 489–520, 2001.

5 Wanninkhof, R., Doney, S. C., Peng, T. H., Bullister, J. L., Lee, K., and Feely, R. A.: Comparison of methods to determine the anthropogenic CO₂ invasion into the Atlantic Ocean, *Tellus*, 51B, 511–530, 1999.

Waugh, D. W., Hall, T. M., McNeil, B. I., Key, R., and Matear, R. J.: Anthropogenic CO₂ in the oceans estimated using transit time distributions, *Tellus B*, 58B, 376–389, doi:10.1111/j.1600-0889.2006.00222.x, 2006.

10

Weiss, R. F., Bullister, J. L., Gammon, R. H., and Warner, M. J.: Atmospheric chlorofluoromethanes in the deep equatorial Atlantic, *Nature*, 314, 608–610, 1985.

BGD

5, 1421–1443, 2008

Anthropogenic CO₂ in the Atlantic Ocean

M. Vázquez-Rodríguez et
al.

Title Page

Abstract

Introduction

Conclusions

References

Tables

Figures

◀

▶

◀

▶

Back

Close

Full Screen / Esc

Printer-friendly Version

Interactive Discussion



Anthropogenic CO₂ in the Atlantic Ocean

M. Vázquez-Rodríguez et
al.

Table 1. Summary statistics for the regions highlighted in Figs. 1b and 2b.

Region	Lat.	Long.	Depth (m)	θ (°C)	Salinity ($\mu\text{mol/kg}$)	pCFC12 (pmol/kg)	Age CFC12 (years)	AOU	$C_{\text{ant}} \Delta C^*$ ($\mu\text{mol/kg}$)	$C_{\text{ant}} \varphi C^*$ ($\mu\text{mol/kg}$)	$C_{\text{ant}} C_{\text{IPSL}}^*$ ($\mu\text{mol/kg}$)	$C_{\text{ant}} \text{TrOCA}$ ($\mu\text{mol/kg}$)	$C_{\text{ant}} \text{TTD}$ ($\mu\text{mol/kg}$)
Deep South Atlantic	20° S–45° S	8° W	>2000	2.0±0.3	34.85±0.04	0.01±0.01	53±4	100.7±11	0.1±0.5	3.3±0.2	0.2±0.5	0.4±1.0	2.8±0.1
N. Subtropical Gyre	20° N–50° N	20° W	100–350	15.6±2.6	36.18±0.43	1.56±0.19	4±4	31.3±21	42.8±0.6	48.7±0.5	50.1±0.9	47.8±0.5	46.1±0.4
S. Subtropical Gyre	20° S–45° S	8° W	100–300	13.1±3.5	35.19±0.46	1.40±0.21	7±2	29.2±18	44.0±0.6	41.3±0.7	52.3±1.0	37.8±0.6	43.8±0.4
Southern Ocean	55° S–72° S	30° E	>500	0.1±0.6	34.68±0.02	0.19±0.13	37±4	125.6±11	1.5±1.6	12.8±0.1	16.4±0.4	11.1±0.2	9.9±0.1
upper Nordic Seas	65–79° N	0–20° W	100–750	–0.2±0.5	34.88±0.05	2.50±0.46	17±4	25.7±12	<i>Null</i>	23.2±1.1	38.2±1.1	24.2±1.2	28.1±0.5
lower Nordic Seas	65–79° N	0–20° W	>1500	–1.0±0.1	34.91±0.01	0.50±0.03	36±3	56.0±5	<i>Null</i>	6.4±0.8	20.9±1.1	4.1±1.2	11.3±0.5
upper DWBC	24° N	50° W–80° W	1200–2200	4.1±0.6	35.02±0.04	0.25±0.17	38±7	61.2±10	21.9±0.5	16.5±0.4	22.1±0.4	21.0±0.5	10.9±0.4
lower DWBC	24° N	60° W–80° W	3200–4200	2.1±0.1	34.91±0.01	0.21±0.10	39±5	57.7±4	6.0±0.6	11.1±0.5	17.3±0.5	9.9±1.0	9.6±0.3

Title Page

Abstract

Introduction

Conclusions

References

Tables

Figures

⏪

⏩

◀

▶

Back

Close

Full Screen / Esc

Printer-friendly Version

Interactive Discussion



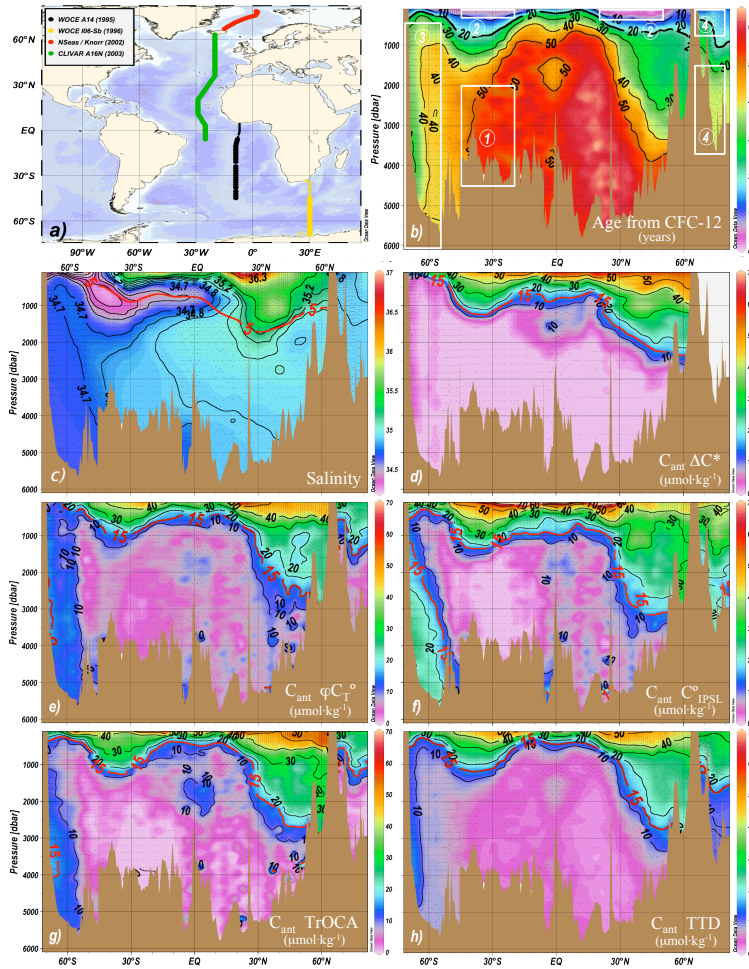


Fig. 1.

Anthropogenic CO₂ in the Atlantic Ocean

M. Vázquez-Rodríguez et al.

Title Page

Abstract

Introduction

Conclusions

References

Tables

Figures

◀

▶

◀

▶

Back

Close

Full Screen / Esc

Printer-friendly Version

Interactive Discussion



Anthropogenic CO₂ in the Atlantic Ocean

M. Vázquez-Rodríguez et
al.

Fig. 1. (a) Map showing the considered meridional cruises WOCE A14, WOCE I06-Sb, CLIVAR A16N and NSeas/Knorr conducted in the Atlantic. Thinner dots in cruises A14 and I06-Sb represent stations not used (latitudinal overlapping of different cruises); **(b)** Age (years) of water masses in the meridional transects from (a), calculated using CFC-12. The inlayed rectangles delimit the regions where C_{ant} estimates are given a closer look, namely: 1=Deep South Atlantic, 2=Northern and southern subtropical gyres, 3=Southern Ocean and 4=The Nordic Seas; **(c)** Salinity distribution of the meridional transect displaying the 5°C isotherm that separates the large volume of cold waters (~86% of the Atlantic Ocean) from warmer surface waters; **(d–h)** Estimates of anthropogenic CO₂ ($\mu\text{mol kg}^{-1}$) in the meridional transect from the ΔC^* , φC_T^o , C_{IPSL}^o , TrOCA and TTD methods, respectively. The red $15 \mu\text{mol kg}^{-1}$ isopleth separates the region of maximum C_{ant} gradient from deeper waters.

Title Page

Abstract

Introduction

Conclusions

References

Tables

Figures

◀

▶

◀

▶

Back

Close

Full Screen / Esc

Printer-friendly Version

Interactive Discussion



Anthropogenic CO₂ in the Atlantic Ocean

M. Vázquez-Rodríguez et al.

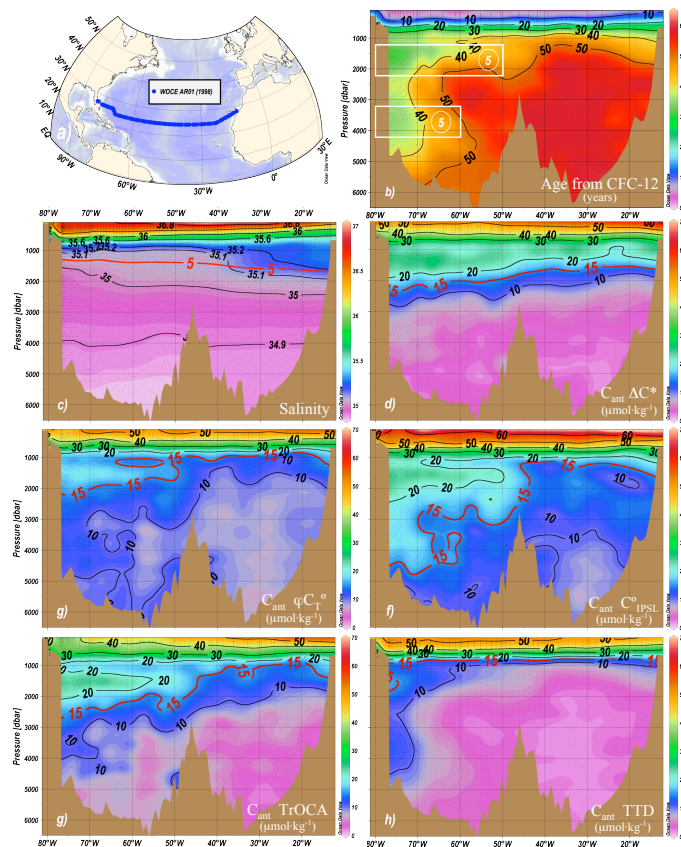


Fig. 2. Analogous contour plots to Fig. 1 for the zonal cruise WOCE AR01. From top to bottom and left to right: **(a)** Cruise map, **(b)** CFC12 Age in years showing the uDWBC and IDWBC limbs in white-contoured boxes numbered as “5”; **(c)** Salinity field with the red 5°C isotherm overlaid; **(d–h)** C_{ant} concentration estimates ($\mu\text{mol kg}^{-1}$) from the ΔC^* , φC_T° , $C^\circ\text{IPSL}$, TrOCA and TTD methods, respectively.

Title Page

Abstract

Introduction

Conclusions

References

Tables

Figures

◀

▶

◀

▶

Back

Close

Full Screen / Esc

Printer-friendly Version

Interactive Discussion



Anthropogenic CO₂ in the Atlantic Ocean

M. Vázquez-Rodríguez et al.

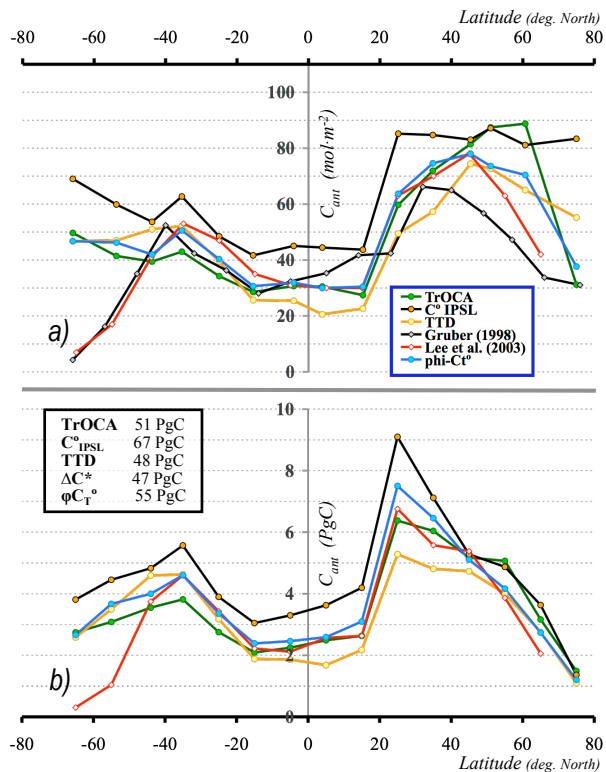


Fig. 3. Specific inventories **(a)** in mol m⁻² for the whole Atlantic computed in latitude bands every 10°, after Lee et al. (2003). The total inventories (Pg C) for the same domain and latitude band resolution are plotted in **(b)**. The inlayed box gives the integrals of the presented total inventories (Pg C) for each method in the Atlantic Ocean.

Title Page

Abstract Introduction

Conclusions References

Tables Figures

◀ ▶

◀ ▶

Back Close

Full Screen / Esc

Printer-friendly Version

Interactive Discussion

